Oropouche virus glycoprotein topology and cellular requirements for virus-like particle assembly

Natalia S. Barbosa[a,b,c], Luis L. P. daSilva[a,b*], Colin M. Crump[c#], Stephen C. Graham[c#]

[a] Center for Virus Research, Ribeirão Preto Medical School, University of São Paulo, Ribeirão Preto, SP, Brazil

[b] Department of Cell and Molecular Biology, Ribeirão Preto Medical School, University of São Paulo, Ribeirão Preto, SP, Brazil

[c] Department of Pathology, University of Cambridge, Cambridge, United Kingdom

[#] Address correspondence to Colin M. Crump, cmc56@cam.ac.uk, or Stephen C. Graham, scg34@cam.ac.uk.

ORCIDs: 0000-0002-2926-5294 (NSB), 0000-0003-3558-0087 (LLPdS), 0000-0001-9918-9998 (CMC), 0000-0003-4547-4034 (SCG)

Running title: Virus-like particle assay for Oropouche virus

Keywords: Bunyavirus, Bunyamwera virus, polyprotein processing, virus budding

Author Contributions: Conceptualization: LLPdS, CMC, SCG; Funding Acquision: NSB, LLPdS, CMC, SCG; Investigation: NSB; Methodology: CMC, SCG; Resources: CMC, SCG; Supervision: LLPdS, CMC, SCG; Visualization: NSB, SCG; Writing – original draft: NSB, SCG; Writing – review & editing: NSB, LLPdS, CMC, SCG.

Word count: 5801 (Abstract: 238; Importance: 150)

Abstract

Oropouche virus (OROV; *Genus: Orthobunyavirus*) is the etiological agent of Oropouche fever, a debilitating febrile illness common in South America. To facilitate studies of OROV budding and assembly, we developed a system for producing OROV virus-like particles (VLPs). Using this system we show that the OROV surface glycoproteins Gn and Gc self-assemble to form VLPs independently of the non-structural protein NSm. Mature OROV Gn has two trans-membrane domains that are crucial for glycoprotein translocation to the Golgi complex and VLP production. Inhibition of Golgi function using the drugs brefeldin A and monensin inhibit VLP secretion, with monensin treatment leading to an increase in co-localisation of OROV glycoproteins with the *cis*-Golgi marker protein GM130. Infection studies have previously shown that the cellular Endosomal Sorting Complexes Required for Transport (ESCRT) machinery is recruited to Golgi membranes during OROV assembly and that ESCRT activity is required for virus secretion. We demonstrate that a dominant negative form of the ESCRT-associated ATPase VPS4 significantly reduces Gn secretion in our VLP assay. Proteasome inhibition using the drug MG132 also disrupts VLPs secretion, suggesting that ubiquitylation promotes ESCRT-mediated VLP release. Additionally, we observe co-localisation between OROV glycoproteins and a specific subset of fluorescently-tagged ESCRT-III components, providing the first insights into which ESCRT-III components are required for OROV assembly. Our *in vitro* assay for OROV VLP production has allowed us to define molecular interactions that promote OROV release and will facilitate future studies of orthobunyavirus assembly.

Importance

Oropouche virus is the etiological agent of Oropouche fever, a debilitating febrile illness common in South America. The tripartite genome of this zoonotic virus is capable of reassortment and there have been multiple epidemics of Oropouche fever in South America over the last 50 years, making Oropouche virus infection a significant threat to public health. However, the molecular characteristics of this arbovirus are poorly understood. We have developed an *in vitro* virus-like particle production assay for Oropouche virus, allowing us to study the assembly and release of this dangerous pathogen without high-containment biosecurity. We determined the polyprotein sites that are cleaved to yield the mature Oropouche virus surface glycoproteins and characterised the cellular machinery required for glycoprotein secretion. Our study provides important insights into the molecular biology of Oropouche virus infection, in addition to presenting a robust virus-like particle production assay that should facilitate future functional and pharmacological inhibition studies.

52 **Introduction**

53 Oropouche virus (OROV) is an arbovirus that is the etiological agent of Oropouche fever, a debilitating
54 febrile illness. Oropouche fever symptoms range from high fever to vomiting, photophobia and, in rare
55 cases, aseptic meningitis or meningoencephalitis (1). OROV is prevalent in the Caribbean and tropical
56 regions of Latin America, and more than 30 epidemics of Oropouche fever have occurred since the first
57 isolation of OROV in 1955 (1). Clinical diagnosis of Oropouche fever is challenging due to the
58 resemblance of its symptoms to diseases caused by other arboviruses like Dengue virus, Zika virus
59 and Chikungunya virus (2). There are no specific antiviral treatments for Oropouche fever, nor is there
60 an effective vaccine to prevent OROV infection. The zoonotic origin, history of human spill-over, tri-
61 segmented RNA genome that is capable of re-assortment (3) and increasing contact between humans
62 and wild-animal reservoirs due to deforestation (1) make OROV a serious epidemic threat.

63 OROV belongs to *Orthobunyavirus* genus of the *Peribunyaviridae* family, one of the twelve families of
64 the order *Bunyavirales*. Orthobunyaviruses form spherical enveloped virus particles that are 100–120
65 nm in diameter and orthobunyavirus genomes comprise three negative sense single-stranded RNA
66 segments: The small segment (S) encodes the nucleocapsid N protein (25–30 kDa), which oligomerizes
67 and encapsidates the viral genome, and the non-structural protein NSs; The medium segment (M)
68 encodes a polyprotein that is post-translationally cleaved by host proteases to yield the viral surface
69 glycoproteins (Gc and Gn) plus a non-structural protein NSm; The large segment (L) encodes the viral
70 RNA dependent RNA polymerase (RdRp) that catalyzes viral replication and transcription. The viral
71 RNA segments are encapsidated by the N protein to form a ribonucleoprotein complex that associates
72 with both the RdRp and the surface glycoproteins to promote virus particle assembly (4). The Gn (~32
73 kDa) and Gc (~110 kDa) glycoproteins are integral membrane proteins with N-terminal ectodomains
74 and they associate in the host endoplasmic reticulum (ER) before being transported to the Golgi
75 complex, the main site of virion assembly (5-7). Studies with Bunyamwera virus (BUNV), the
76 prototypical orthobunyavirus, have shown that the virus particles undergo distinct morphological
77 changes inside Golgi and *trans*-Golgi network cisternae (6), and studies of both BUNV and OROV have
78 shown profound fragmentation of Golgi complex cisternae during virus infection of some cell types (5,
79 6).

80 OROV assembly at the Golgi complex is stimulated by the cellular Endosomal Sorting Complexes
81 Required for Transport (ESCRT) machinery (5). The ESCRT machinery mediates membrane
82 deformation and scission in an 'inside-out' topology, in contrast to the 'outside-in' topology of endocytic
83 vesicles (8). The human ESCRT machinery comprises multiple distinct protein complexes (ESCRT-0,
84 ESCRT-I, ESCRT-II and ESCRT-III) plus several accessory proteins, with final membrane scission
85 being promoted by the concerted action of ESCRT-III and the ATPase VPS4 (9). The ESCRT-III
86 machinery is formed by members of the charged multivesicular body protein (CHMP) family, with distinct
87 CHMP proteins playing specific coordinated roles. The first ESCRT-III component recruited is CHMP6,
88 which recruits CHMP4 isotypes (CHMP4A or CHMP4B) to homo-oligomerizes at the target membrane.
89 The CHMP2A plus CHMP3 complex and/or CHMP2B alone are then recruited, activating VPS4 to

90 promote ESCRT-III filament disassembly and membrane scission (9-11). Virus recruitment of the
91 ESCRT-III machinery is canonically mediated by direct association of viral 'late domains' with ESCRT-
92 I, the cellular ubiquitylation machinery and/or the accessory protein ALIX. These interactions culminate
93 in recruitment and activation of the ESCRT-III machinery (12, 13). With the exception of flaviviruses,
94 which recruit ESCRT components to the ER (14), most viruses recruit ESCRT machinery to the plasma
95 membrane, endosomes or other 'post-Golgi' membranes (13, 15). It is therefore particularly interesting
96 that OROV budding involves direct recruitment of ESCRT machinery to Golgi membranes (5). The
97 OROV glycoproteins do not contain any identifiable viral 'late domains' and the molecular basis of
98 ESCRT machinery recruitment by OROV thus remains to be established.

99 The study of virus assembly and budding is greatly aided by recombinant technology to generate virus-
100 like particles (VLPs), which are released by cultured cells expressing specific virus components and
101 are genome-free but otherwise structurally resemble authentic virus particles. Recombinant VLP
102 systems facilitate investigation of highly-pathogenic virus assembly pathways under reduced biosafety
103 containment (16, 17) and VLPs have been widely used as tools for vaccine development (18). VLP
104 production systems have been established for several members of the order *Bunyavirales*, with
105 phlebovirus and hantavirus VLP assembly requiring expression of the viral glycoproteins but not the
106 nucleoprotein (19, 20). While a mini-replicon system has been reported for BUNV and OROV (21, 22),
107 no VLP system has been established to study orthobunyavirus assembly and budding.

108 Here we report production of OROV VLPs via recombinant expression of the M polypeptide. We
109 observe that the M polyprotein yields a mature Gn protein containing two transmembrane domains that
110 are crucial for viral glycoprotein targeting to the Golgi complex and for VLP production. We show that
111 pharmacological disruption of Golgi function prevents OROV VLP secretion, as does perturbation of
112 ESCRT function, which highlights the utility of this VLP production assay for probing cellular
113 determinants of OROV assembly. Finally, we show co-localisation of ESCRT components with Gn and
114 Gc in cells, giving insights into the cellular factors that sustain OROV assembly and release.

115

116 **Results**

117 *OROV virus-like particle characterization*

118 The middle (M) segment of the OROV genome (residues 1–1420) was cloned as a cDNA fragment into
119 the mammalian expression vector pcDNA3.1 with an HA epitope tag between the secretion signal
120 sequence (SS) and the first residue of the mature Gn protein (Fig. 1A). Transfection of HEK293T cells
121 with HA-tagged OROV M polyprotein yielded high levels of Gn and Gc (observed as bands at ~35 kDa
122 and ~120 kDa, respectively) in the supernatant, consistent with the production of OROV virus-like
123 particles (VLPs) by these transfected cells (Fig. 1B). In order to establish whether both OROV
124 glycoproteins are required for VLP production, OROV Gn (M segment residues 1–312) and Gc (M
125 segment residues 481–1420) were cloned separately into pcDNA3.1 with an N-terminal secretion signal
126 and HA epitope tag (Fig. 1A), the polypeptide cleavage sites being inferred from homology with those
127 determined or predicted for the Bunyamwera M polyprotein (23). As expected, neither Gn nor Gc was
128 abundant in the cell supernatant when transfected into HEK293T cells in isolation. However, we also
129 failed to observe secreted glycoproteins when the proteins were co-expressed (Fig. 1B). This was
130 unexpected as a previous study of OROV infection had shown that the NSm polypeptide, which lies
131 between Gn and Gc in the M polyprotein, was dispensable for virion production (24). Furthermore, we
132 observed that HA-tagged Gn from cells transfected with a plasmid encoding HA-tagged M polypeptide
133 migrated more slowly in SDS-PAGE than Gn from cells transfected with the HA-Gn plasmid (Fig. 1B),
134 consistent with the two proteins having different masses. Analysis of the OROV M polypeptide
135 sequence using the SignalP 5.0 server (25) suggested that the cleavage site which liberates Gn from
136 the M polypeptide may lie between residues G335 and E336 (Fig. 1A, second arrow), thus yielding a
137 mature Gn protein with two trans-membrane domains (TMDs). A second HA-tagged Gn expression
138 construct that included this extra TMD was thus generated (GnX; residues 1-339). While GnX was not
139 secreted into the medium following transfection on its own into HEK293T cells, both GnX and Gc were
140 abundant in the supernatant of cells co-transfected with constructs encoding both proteins (Fig. 1C).
141 This suggested that co-expression of Gc with GnX is sufficient to stimulate production of VLPs, VLP
142 production requiring Gn to encompass the first two TMDs of the M polyprotein. To test whether the two
143 TMDs plus cytosolic region of GnX (residues 203–339; GnCTX) were sufficient to promote Gc secretion,
144 and thus VLP production, HEK293T cells were co-transfected with GnCTX and Gc expression
145 constructs. Neither Gc nor GnCTX was secreted to the supernatant of these co-transfected cells,
146 indicating that GnCTX is not sufficient to promote secretion of Gc (Fig. 1C). Taken together, these
147 results demonstrate that OROV VLPs are formed following co-expression of the surface glycoproteins,
148 either as individual proteins or as a polyprotein, but that the M polyprotein is cleaved after the second
149 TMD to liberate the mature OROV Gn protein (GnX).

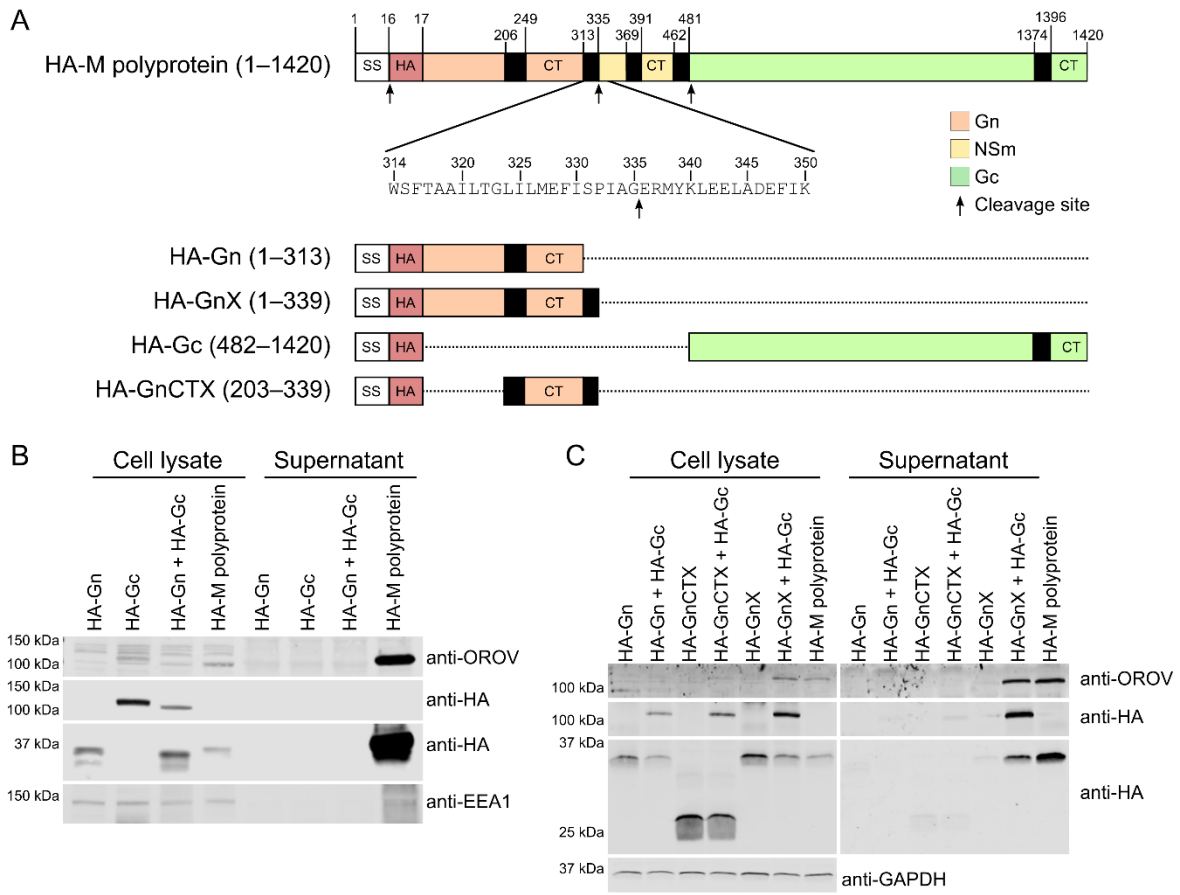

Figure 1. Recombinant production of OROV virus-like particles. (A) Schematic representation of the recombinant constructs used to express the OROV M polyprotein, individual glycoproteins or domains thereof. All expression constructs were preceded by the OROV M signal sequence (SS; unshaded) and an HA epitope tag (HA; red shading). Regions corresponding to Gn, Gc and the NSm non-structural protein are shaded in orange, green and yellow, respectively, with cytosolic tails denoted (CT). Predicted transmembrane regions (black) and polypeptide cleavage sites (arrows) are shown. (B and C) HEK293T cells were transfected with HA-tagged OROV M (poly)protein constructs. After 48 h cell lysates and supernatants were harvested, subjected to SDS-PAGE and immunoblotted using anti-HA and anti-OROV antibodies to detect secreted proteins, the latter polyclonal antibody detecting Gc but not Gn, and with anti-EEA1 (B) or anti-GAPDH (C) antibodies used as loading controls.

The GnX:Gc complex is sufficient for Golgi localization

During infection, the orthobunyavirus M segment is translated at the ER before the Gn and Gc proteins are transported to the Golgi apparatus, which is the main site of virus assembly (4). In order to investigate the subcellular distribution of recombinant OROV glycoproteins (Fig. 1A), HeLa cells were transfected with HA-tagged OROV glycoproteins and then stained for the HA signal and for the ER chaperone calnexin 2 (CNX2) or the *cis*-Golgi marker GM130 (Fig. 2). When expressed alone, HA-tagged Gn, Gc and GnX all co-localized with CNX2 at the ER and did not co-localise with GM130 at the Golgi (Fig. 2A–C). Similarly, when HA-tagged Gn and Gc were co-expressed they were retained at the ER and did not co-localise at the Golgi (Fig. 2D). However, when HA-tagged GnX and Gc were co-expressed they showed extensive co-localisation with GM130 at the Golgi and less-extensive co-localisation with CNX2 at the ER (Fig. 2E). Extensive GM130 co-localisation was also observed when

172 the HA-tagged OROV M polyprotein was expressed (Fig. 2F). Additionally, HA-stained punctae could
173 often be observed outside cells expressing the M polyprotein (Fig. 2F), consistent with the production
174 of VLPs that remain adhered to the coverslip during fixation and subsequent preparation of the
175 microscope slides. Taken together, these data suggest that co-expression of Gn spanning the first two
176 predicted TMDs (residues 1–339; GnX) with Gc, either as separate polypeptides or as a polyprotein, is
177 necessary and sufficient for these proteins to be transported from the ER to the Golgi apparatus.

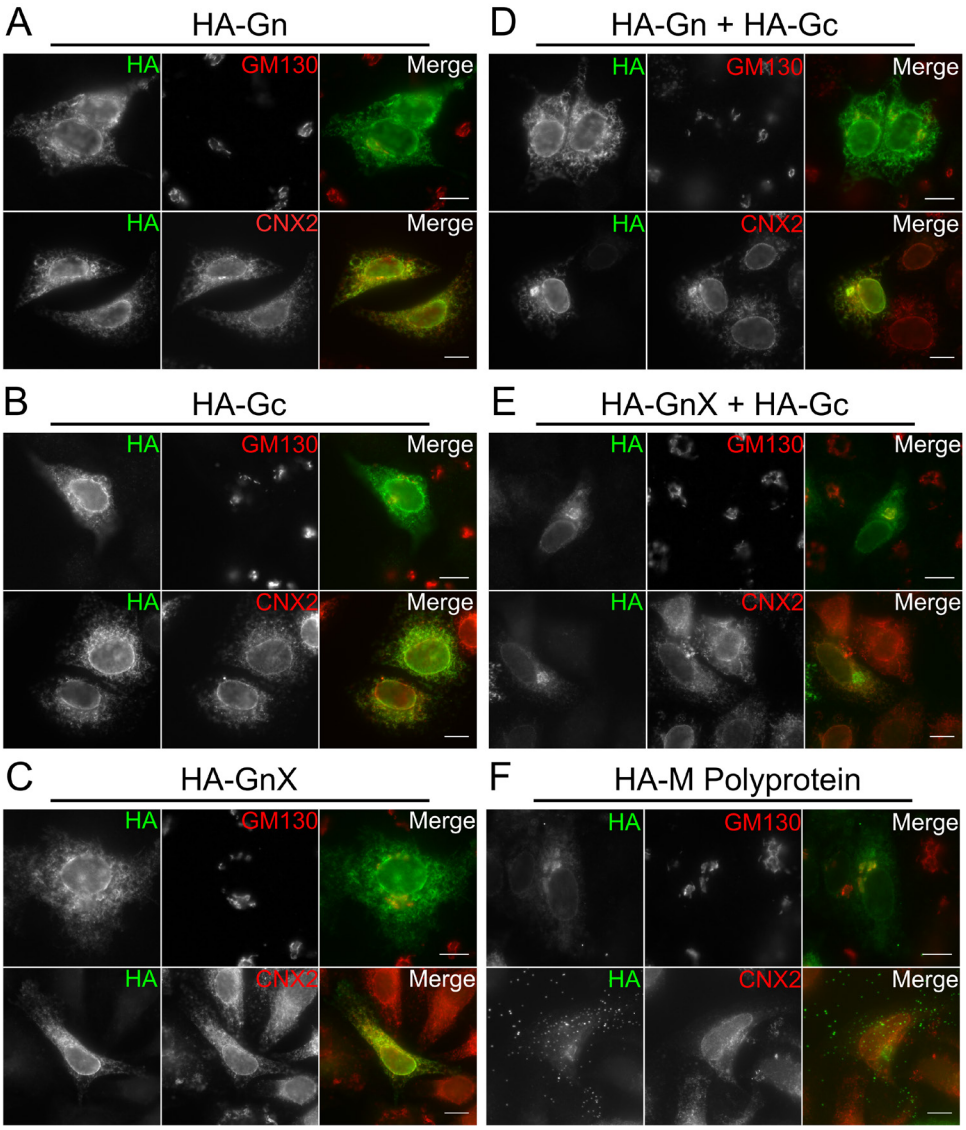

178

179 **Figure 2. Intracellular localization of OROV glycoproteins.** HeLa cells were transfected with
180 plasmids expressing the HA-tagged OROV glycoproteins or the M polyprotein (as indicated). Cells were
181 fixed and co-stained with rabbit anti-HA (AF488) and either mouse anti-GM130 (AF568) or mouse anti-
182 CNX2 (AF568) antibodies before analysis using wide-field fluorescence microscopy. Bars = 10 μm.

183 *Inhibition of the post-Golgi transport disrupts OROV glycoprotein secretion*

184 The OROV assembly pathway involves the recruitment of the host ESCRT machinery to Golgi
185 membranes for virus particle production (5). To further investigate the intracellular trafficking of the
186 OROV M polyprotein, drugs that interfere with different cellular trafficking pathways were utilised. Golgi

187 transport was disrupted at two different steps: Brefeldin A was used to inhibit ER to Golgi transport, and
188 monensin was used to block post-Golgi transport (26, 27). As some ESCRT components recognise
189 partner proteins by interacting with ubiquitin, we also incubated cells with the proteasome inhibitor
190 MG132, which depletes cellular mono-ubiquitin by preventing the recycling of ubiquitin that occurs when
191 ubiquitylated proteins are degraded by the proteasome (28). HEK293T cells were transfected with HA-
192 tagged OROV M and the culture medium was collected before and after drug treatment to monitor
193 glycoprotein secretion. Secretion of OROV glycoproteins was strongly reduced in cells treated with
194 MG132 and was completely disrupted in cells treated with monensin or brefeldin A (Fig. 3A).
195 Interestingly, only treatment with monensin led to an increase of glycoprotein abundance in the treated
196 cell lysates (Fig. 3A). Microscopic analysis of drug-treated HeLa cells (Fig. 3B) showed that brefeldin A
197 caused dispersal of the *cis*-Golgi marker GM130 and prevented co-localisation of GM130 with the
198 OROV glycoproteins. Conversely, monensin treatment led to an enlarged GM130-positive structure that
199 strongly co-localised with the OROV glycoprotein HA signal. There was no obvious difference in the
200 distribution in GM130 staining or its co-localisation with the OROV glycoprotein HA signal in cells mock-
201 treated or treated with the proteasome inhibitor MG132. These results demonstrate that glycoprotein
202 secretion is inhibited when the Golgi apparatus or ubiquitin/proteasome system are disrupted, and that
203 treatment of cells with monensin causes accumulation of OROV glycoproteins at GM130 positive
204 compartments.

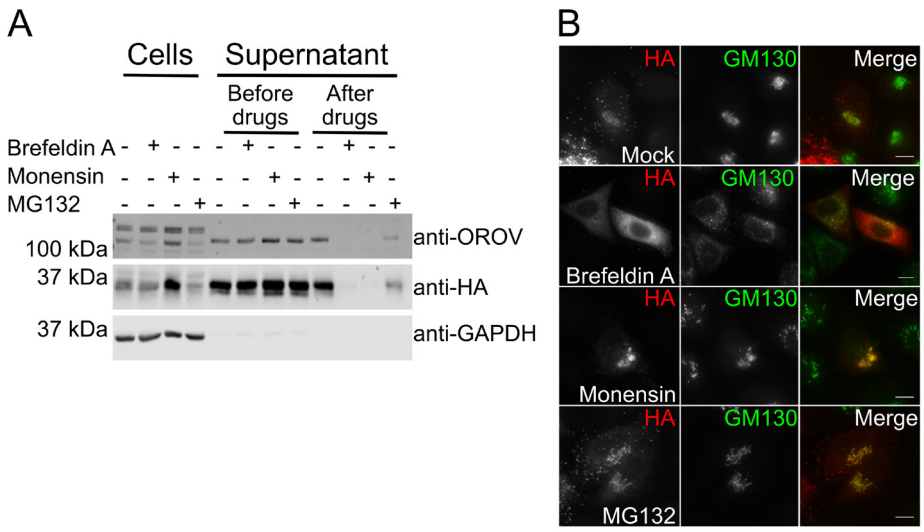

205

206 **Figure 3. Disruption of the Golgi apparatus or proteasome prevents OROV VLP secretion.** (A)
207 HEK293T cells were transfected with HA-tagged OROV M polyprotein and after 18 h the cell
208 supernatant was harvested and reserved. The culture medium was replenished and supplemented with
209 the drugs brefeldin A, monensin or MG132, or with an equivalent amount of DMSO (mock). After 6h of
210 drug treatment, cells and supernatant were harvested. All samples were then subjected to SDS-PAGE
211 and immunoblotted using anti-HA and anti-OROV antibodies, with anti-GAPDH used as a loading
212 control. (B) HeLa cells transfected and treated as (A). After drug treatment the cells were fixed and co-
213 stained with rabbit anti-HA (AF568) and mouse anti-GM130 (AF488) antibodies before analysis using
214 wide-field fluorescence microscopy. Bars = 10 μm.

215 *Production of OROV VLPs requires ESCRT machinery*

216 During OROV infection, multiple ESCRT components are recruited to Golgi membranes in order to
217 promote virus particle production (5). VPS4 is a cellular ATPase that stimulates the disassembly of
218 assembled ESCRT-III filaments at the necks of vesicles budding away from the cytoplasm, promoting
219 membrane scission (9). VPS4 is recruited to Golgi membranes during OROV infection and the
220 morphology of OROV viral factories is altered when infected cells express a dominant negative form of
221 this enzyme (VPS4E/Q) that inhibits ESCRT-III disassembly (5). In order to analyse whether production
222 of OROV VLPs is ESCRT-dependent, HEK293 cells stably expressing GFP-tagged wild-type or
223 dominant negative VPS4 under the control of ecdysone response elements (29) were transfected with
224 HA-tagged OROV M segment. Following transfection of these VPS4-expressing cells, or the parental
225 HEK293 cells not expressing VPS4, the cells were treated with either ponasterone A (Pon A) to induce
226 VPS4 expression, or with DMSO as a vehicle control, and the amount of secreted Gn and Gc was
227 monitored by immunoblotting (Fig. 4A). The secretion of Gn and Gc by parental cells and those
228 expressing wild-type GFP-VPS4 did not significantly differ when cells were treated with Pon A or DMSO
229 (Fig 4B). Gn and Gc secretion was decreased when GFP-VPS4E/Q cells were treated with Pon A,
230 although only the decrease in Gn was statistically significant (Fig. 4B). Similar to previous observations
231 in OROV-infected HeLa cells (5), in Pon A treated cells OROV glycoproteins and GFP-tagged Vps4E/Q
232 co-localised near to GM130-containing Golgi membranes (Fig. 4C). However, unlike previous studies
233 of OROV-infected cells, we did not observe extensive co-localisation of GFP-tagged wild-type VPS4
234 with either the OROV glycoproteins nor the Golgi marker GM130.

235 To further investigate the interaction between ESCRT-III components and OROV glycoproteins, HeLa
236 cells were transiently co-transfected with HA-tagged OROV M segment and dominant-negative
237 C-terminally YFP/GFP tagged members of the charged multivesicular body protein (CHMP) family (30).
238 Co-localization could clearly be observed between OROV glycoproteins and CHMP6-YFP, CHMP4A-
239 YFP, CHMP4B-YFP, CHMP2A-YFP or CHMP1A-YFP (Fig. 4D). These co-localised proteins were near
240 to GM130-positive Golgi membranes, although the overlap between the HA/YFP and GM130 signals
241 was not extensive (Fig. 4D). In contrast, there was no apparent co-localization between OROV
242 glycoproteins and CHMP2B-GFP or CHMP3-YFP (Fig. 4D). These data show that multiple ESCRT-III
243 components associate with OROV glycoproteins and suggest that ESCRT-III activity is required for
244 efficient VLP formation, as has been observed for production of OROV virus particles in infected cells.

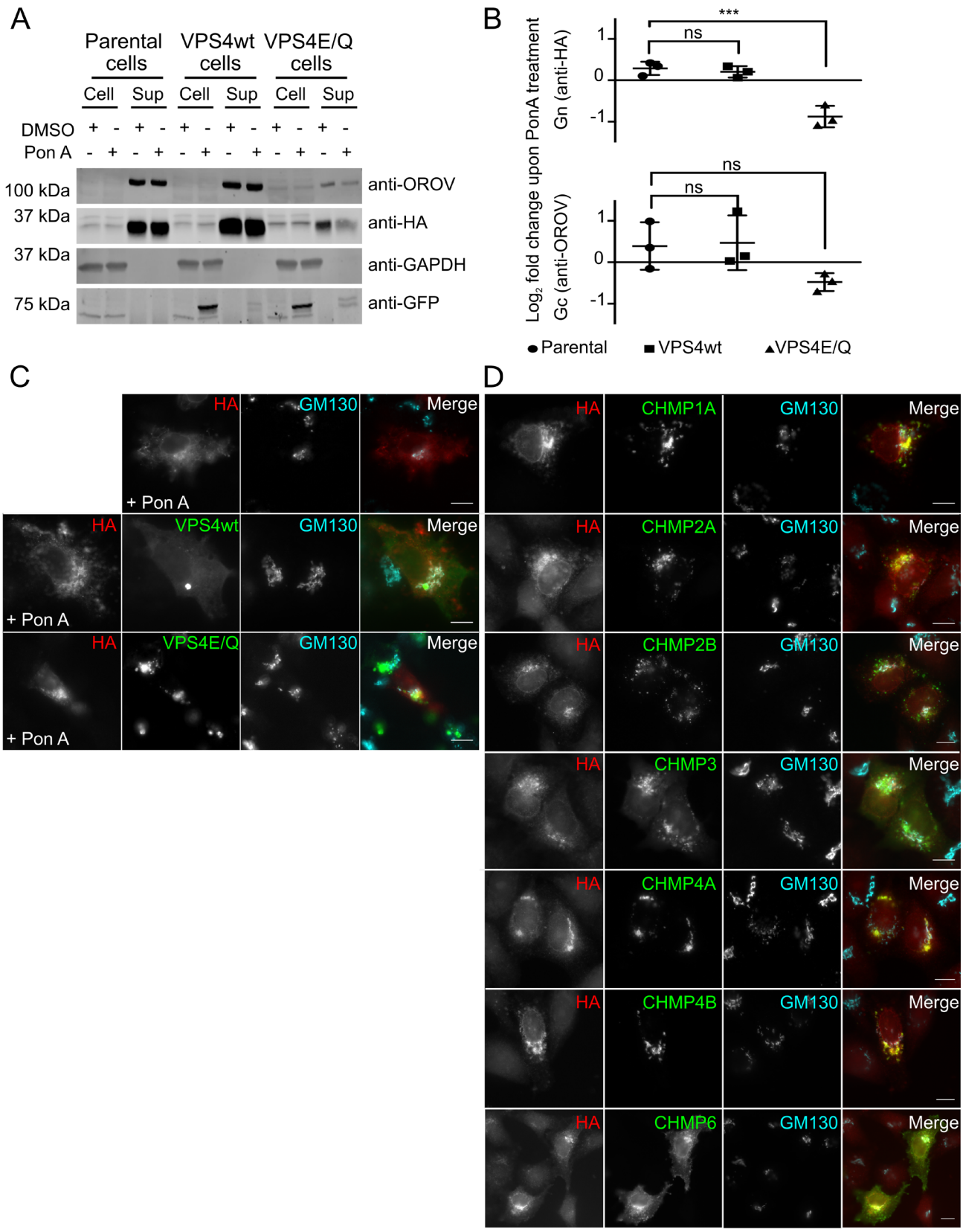

Figure 4. Interaction of OROV glycoproteins with cellular ESCRT machinery. (A) HEK293 cells stably expressing GFP-tagged wild-type VPS4 (VPS4wt) or a dominant negative mutant (VPS4E/Q) under the control of the ecdysone response element, or parental cells as a control, were transfected with HA-M segment and treated with either 1 µM ponasterone A (Pon A) or with DMSO as a control.

250 After 48 h, cells (*Cell*) and supernatant (*Sup*) were harvested, subjected to SDS-PAGE and
251 immunoblotted using anti-GFP, anti-HA and anti-OROV antibodies, with anti-GAPDH used as a loading
252 control. (B) Quantitation of fold change in Gn (anti-HA; upper panel) and Gc (anti-OROV; lower panel)
253 secretion upon ponasterone A treatment. The $\log_2$ ratio of protein in the supernatant of ponasterone A-
254 treated cells versus cells treated with DMSO is shown for three independent experiments. Bars
255 represent the mean ± SD. ***, $p < 0.005$ (One-way ANOVA using Dunnett's test for multiple comparisons
256 to parental control cells). (C) HEK293 cells expressing GFP-VPS4wt or GFP-VPS4E/Q, or parental
257 cells, were transfected with HA-tagged OROV M segment and treated with 1 μM ponasterone A for 18
258 h before being fixed and co-stained with rabbit anti-HA (AF568) and mouse anti-GM130 (AF647)
259 antibodies and then analysed by wide-field fluorescence microscopy. Bars = 10 μm. (D) HeLa cells
260 were co-transfected with plasmids expressing HA-tagged OROV M segment and YFP/GFP-tagged
261 ESCRT-III components (as indicated). After 18 h, cells were fixed and co-stained with rabbit anti-HA
262 (AF568) and mouse anti-GM130 (AF647) before being analysed by wide-field fluorescence microscopy.
263 Bars = 10 μm.

264 **Discussion**

265 In this present work we have characterized the production of Oropouche virus-like particles (VLPs) as
266 a tool to study OROV assembly and budding. It has been reported for other members of the order
267 *Bunyavirales* that the surface glycoproteins are the main viral components necessary for VLP
268 production (19, 20). Here, we showed that OROV VLPs are formed when Gn and Gc are co-expressed,
269 with the proteolytic processing of OROV Gn differing from that of other orthobunyaviruses, that VLP
270 production is inhibited by drugs that interfere with Golgi or proteasome function, and that the cellular
271 ESCRT machinery is required for efficient VLP production.

272 Previous studies of BUNV have shown two cleavage sites between the boundaries of Gn and NSm in
273 the M polyprotein, either side of the second TMD (23). Specifically, Shi and colleagues (23) observed
274 that the second TMD of the BUNV M polyprotein (which they term NSm^{SP}) acts as a signal peptide for
275 NSm, being cleaved at its C terminus by cellular signal peptidases, and that this TMD is subsequently
276 liberated from the mature Gn protein by signal peptide peptidase. In contrast, we show that this second
277 TMD (which we term X) is retained by the mature OROV Gn protein. Shi and colleagues (23) also
278 observed that the migration of the BUNV Gn protein in SDS-PAGE changed linearly when Gn was
279 truncated before the start of the second TMD. However, when stop codons were introduced at or
280 following the start of this second TMD the resultant Gn protein migrated identically to mature Gn protein
281 arising from BUNV infection or M polyprotein expression. In contrast, we observe that the migration of
282 HA-tagged Gn OROV (residues 1–313), containing only one TMD, differs from that of HA-tagged Gn
283 obtained when the entire OROV M polyprotein is expressed (Fig 1B, C). However, the migration of HA-
284 tagged GnX (residues 1–339) matched that of the mature HA-tagged Gn protein obtained via M
285 polyprotein processing (Fig 1C). Furthermore, we observe the efficient secretion of OROV glycoproteins
286 into the culture medium, presumably as VLPs, when GnX (residues 1–339) is co-expressed with Gc or
287 when the OROV M segment is expressed as a single polyprotein, but not when Gn (residues 1–313) is
288 co-expressed with Gc. Taken together, these data show that a mature Gn protein spanning two TMDs
289 (GnX) is produced when the OROV M polyprotein is processed, in contrast to previous observations for
290 BUNV, and we conclude that the requirement for cleavage of the second TMD from Gn by signal peptide
291 peptidase differs across orthobunyaviruses.

292 In addition to differences in proteolytic processing of the M polypeptide between BUNV and OROV, we
293 observed a difference in the requirement for co-expression of Gn and Gc in order for these proteins to
294 traffic from the ER to the Golgi. Previous studies have shown that the Gn protein of BUNV is trafficked
295 to the Golgi complex when expressed alone (7), due to the Golgi retention signal located on its first
296 TMD (31). In contrast, we observe that neither Gn with either one or two TMDs (Gn and GnX,
297 respectively) nor Gc localise to the Golgi when expressed in isolation (Fig. 2). When Gc was co-
298 expressed with Gn (one TMD), both proteins were still retained in the ER, whereas co-expression of Gc
299 with GnX (two TMDs) resulted in strong co-localisation of the glycoproteins with the Golgi marker
300 GM130. We observed similar co-localisation of the OROV glycoproteins with GM130 when expressing
301 the entire M polyprotein. Taken together, these results confirm the requirement of the second Gn TMD
302 for correct protein function. The difference in requirement for Gn and Gc co-expression in order to
303 mature beyond the ER into the Golgi may highlight structural differences between the orthobunyavirus
304 glycoproteins, with the BUNV Gn extracellular domain being capable of folding independently whereas
305 the OROV Gn extracellular region requires Gc for folding and/or stabilisation.

306 Since Bunyavirus do not possess a matrix protein, the cytosolic tails of Gn and Gc are believed to be
307 important for virus assembly and budding. The Gn cytosolic domain of Uukuniemi phlebovirus interacts
308 with the virus ribonucleoprotein, which is crucial for genome packaging (32), and previous studies of
309 BUNV showed the Gn and Gc cytosolic tails to be required for Golgi complex targeting, virus assembly
310 and infectivity (33). Furthermore, it has been shown that the first TMD of BUNV Gn is required for correct
311 Golgi targeting of Gc (31). We therefore investigated whether the Gn cytosolic tail (GnCTX) could serve
312 as a chaperone for Gc. We observed that Gc is not secreted into the medium when co-expressed with
313 GnCTX, suggesting that VLPs were not being correctly formed, whereas co-expression of Gc with GnX
314 did promote glycoprotein secretion (Fig 1C). This data confirms that the Gn extracellular domain is
315 required for secretion of Gc, consistent with previous studies of BUNV showing that mutations in the
316 glycosylation sites of Gn prevented correct folding of both Gn and Gc (34).

317 Previous studies of BUNV showed that budding and initial maturation steps occur in the Golgi stacks,
318 but that full virus maturation does not proceed without a functional *trans*-Golgi (6). Fragmentation of the
319 Golgi is observed when Vero cells are infected with BUNV, although these fragmented Golgi are still
320 competent to sustain infectious virion production (6). Similarly, OROV infection leads to *trans*-Golgi
321 network fragmentation as detected by dispersion of the TGN46 marker (5). We do not observe
322 fragmentation of the Golgi in cells expressing the M polyprotein (Fig. 2F and 3B), suggesting that
323 additional OROV proteins are required to promote Golgi fragmentation. In order to investigate the
324 intracellular trafficking of OROV VLPs, we used two drugs that interfere with the Golgi complex in
325 different manners. The drug monensin strongly disrupts *trans*-Golgi network function by altering the pH
326 (27), allowing us to probe post-Golgi transport of VLPs (Figure 3). We observed an accumulation of
327 glycoproteins at GM130-positive compartments in monensin-treated cells with a concomitant drop in
328 glycoprotein secretion into the extracellular medium, confirming that a functional *trans*-Golgi network is
329 required for OROV VLP secretion. Brefeldin A prevents protein traffic from the ER to the Golgi but
330 allows retrograde trafficking to proceed, causing re-adsorption of the Golgi into the ER (35). As

331 expected, we observed a loss of the distinct Golgi-like staining patterns for both the OROV glycoproteins
332 and the *cis*-Golgi marker GM130, plus a loss of VLP secretion, following brefeldin A treatment.
333 Interestingly, we do not observe accumulation of intracellular glycoproteins, consistent with a loss in
334 protein translation caused by the ER stress induced by brefeldin A treatment (36). Taken together, our
335 data show that disruption of Golgi function inhibits OROV VLPs production, as has been observed
336 previously for cells infected with BUNV (37).

337 The production of OROV infectious particles requires the cellular ESCRT machinery (5). To probe
338 whether OROV VLP production also requires ESCRT activity, and thus faithfully recapitulates infectious
339 virus particle production, we investigated the association of ESCRT components with OROV
340 glycoproteins and the requirement of ESCRT machinery for VLP production. Exploitation of the cellular
341 ESCRT machinery by retroviruses requires the small protein ubiquitin (13), with retrovirus budding
342 being inhibited when free ubiquitin is depleted from cells by means of proteasomal inhibition (38). We
343 observe that secretion of OROV VLPs is strongly reduced in cells treated with the proteasomal inhibitor
344 MG132 (Fig. 3), consistent with a role for ubiquitin and the ESCRT machinery in VLP secretion. The
345 ESCRT-III–disassembling ATPase VPS4 has previously been shown to co-localise with OROV
346 replication sites, with expression of the ATPase-defective VPS4E/Q mutant leading to changes in
347 replication compartment morphology (5). We observe that the secretion of OROV VLPs is decreased
348 from cells expressing VPS4E/Q, whereas secretion from parental cells or those expressing wild-type
349 VPS4 is unchanged (Fig. 4A, B). This decrease in secretion is statistically significant when quantitating
350 HA-tagged Gn ($p = 0.0006$), whereas there is a consistent but not statistically significant decrease when
351 quantitating Gc using anti-OROV ($p = 0.1451$). We are unable to explain this discrepancy except to
352 note that the anti-HA staining of Gn was more consistent across experiments than the anti-OROV
353 staining of Gc, potentially due to higher detection efficiency afforded by the monoclonal anti-HA
354 antibody or more consistent electrophoretic transfer of the smaller Gn protein to nitrocellulose
355 membranes. We also note that glycoprotein secretion was generally poorer in unstimulated VPS4E/Q
356 expressing cells (Fig 4A), potentially due to an undetectable level of 'leaky' expression of the VPS4E/Q
357 mutant in unstimulated cells that would reduce the dynamic range afforded by this assay. Interestingly,
358 while GFP-VPS4E/Q co-localized with OROV glycoproteins at Golgi membranes in a similar manner
359 as OROV infectious particles (5), GFP-VPS4wt did not (Fig. 4). This suggests that additional OROV
360 proteins are required for stable recruitment of VPS4 to OROV glycoproteins.

361 To further understand how cellular ESCRT components may promote OROV VLP production, we
362 investigated the co-localisation of OROV glycoproteins with overexpressed, dominant-negative
363 YFP/GFP-tagged cellular ESCRT-III components. CHMP6, a component known to initiate ESCRT-III
364 polymers (8), co-localises with OROV glycoproteins, as do the polymerising ESCRT-III components
365 CHMP2A and all isoforms of CHMP4 (Fig. 4). However, we don't observe co-localisation of CHMP2B
366 (Fig. 4). CHMP2B displays affinity for $PI(4,5)P_2$ and is known to be required for formation of long-lived
367 ESCRT-III complexes involved in the morphogenesis and maintenance of dendritic spines (39). Both
368 CHMP2A and CHMP2B can contribute to HIV-1 budding, with loss of both leading to severe defects in
369 virus assembly (40). On face value, our data suggest that OROV VLP production is likely to depend

370 more strongly on CHMP2A rather than CHMP2B. However, CHMP3 was not observed to co-localise
371 with OROV glycoproteins (Fig. 4D) and previous experiments with HIV suggest that CHMP2A-mediated
372 stimulation of virus budding requires CHMP3 (11). Further experiments will be required in order to
373 determine which CHMP2 isoform stimulates OROV budding, and whether CHMP3 participates in this
374 activity.

375 In summary, we have demonstrated that OROV Gn contains two transmembrane domains essential for
376 OROV glycoprotein trafficking to the Golgi complex. Pharmacological disruption of Golgi function
377 inhibits OROV VLP secretion, as does perturbation of ESCRT complex function. Furthermore, we
378 observe co-localisation of only selected CHMP-family ESCRT-III components with the OROV
379 glycoproteins, giving initial insights into the cellular requirements for virus budding. We anticipate that
380 our OROV VLP production assay will facilitate future studies on bunyavirus assembly and budding, and
381 accelerate attempts to develop vaccines against OROV and/or identifying novel antiviral drugs that
382 prevent Oropouche fever.

383 **Materials and Methods**

384 *Cell Culture*

385 Mycoplasma-free HeLa and HEK293T cells were maintained in Dulbeco's modified Eagle's medium
386 (DMEM; Gibco) supplemented with 10% heat-inactivated foetal calf serum and 2 mM glutamine at 37°C
387 in a humidified 5% CO_2 atmosphere. HEK293 cells stably expressing the ecdysone receptor (EcR-293;
388 Invitrogen), and derived cell lines stably expressing GFP-tagged wild-type or dominant negative VPS4
389 under the control of ecdysone response elements, were maintained in the medium listed above
390 supplemented with 400 µg/ml Zeocin and 800 µg/ml G418 (29).

391 *Plasmids and Constructs*

392 All fragments of the M polyprotein from OROV strain BeAn19991 (GenBank ID KP052851.1) used in
393 this study were synthesised (GeneArt) following codon-optimization for expression in human cells.
394 Constructs encoding Gn (M polyprotein residues 1–313) and Gc (residues 482–1420) were synthesised
395 with an HA epitope tag and BamHI restriction sequence immediately following the Gn signal sequence
396 (SS), and were cloned into pcDNA3.1(+) using the restriction enzymes NheI and XhoI. To generate the
397 HA-tagged OROV M polypeptide construct, an extended NSm fragment (M polyprotein residues 299–
398 496) was synthesised to overlap with the N and C termini of Gc and Gn, respectively. The sequences
399 for Gc, NSm and the entire pcDNA3.1 vector encoding Gn with an N-terminal signal sequence plus HA
400 tag were amplified by PCR using KOD Hot Start DNA polymerase (Novagen) using the primers shown
401 in Table 1, mixed and then concatenated using the NEBuilder HiFi assembly kit according to the
402 manufacturer's instructions to yield pSnH-OROV-M. HA-tagged GnX was generated by site directed
403 mutagenesis of pSnH-OROV-M to insert a stop codon after residue 339 using the mutagenic primers
404 listed in Table 1. HA-tagged GnCTX was amplified from pSnH-OROV-M using the primers shown in
405 Table 1, digested with the restriction endonucleases BamHI and XhoI, and ligated into BamHI/XhoI

406 digested pSnH-OROV-M to yield the Gn signal sequence and an HA epitope tag followed by M
407 polypeptide residues 203–339. All expression constructs were verified by Sanger sequencing. CHMP-
408 YFP/GFP plasmids were as described previously (30).

409 *Table 1. Oligonucleotide primers used in this study. Restriction sites are in **bold**.*

Name	Sequence (5′ to 3′)	Details
Gn C-terminal forward	CAAGAGCCTGAGCAAGGCCAG	Amplify NSm to generate HA-M polyprotein construct
Gc N-terminal reverse	CTTGGTAGGTGATCTTGATGTCCTTGC	Amplify NSm to generate HA-M polyprotein construct
pcDNA 3′ forward	CGTTTAAACCCGCTGATCAGC	Amplify Gn and pcDNA vector to generate HA-M polyprotein construct
Gn C-terminal reverse	GCTCTTGCTCTTGCACATCTGTC	Amplify Gn and pcDNA vector to generate HA-M polyprotein construct
Gc N-terminal forward	GATGAGGACTGCCTGAGCAAGGAC	Amplify Gc to generate HA-M polyprotein construct
BGH reverse	TAGAAGGCACAGTCGAGG	Amplify Gc to generate HA-M polyprotein construct
GnX forward	CGAGCGGATGTACTAGCTGGAAGAACTG	Generate GnX by replacing reside 340 of HA-M polyprotein with a stop codon
GnX reverse	CAGTTCTTCCAGCTAGTACATCCGCTCG	Generate GnX by replacing reside 340 of HA-M polyprotein with a stop codon
GnCTX forward	GAA**GGATCC**GAGGCTATGTGCGTGAACATC	Clone HA-tagged GnCTX
GnCTX reverse	GGAA**CTCGAG**TCAGTACATCCGCTCGCCGGC AATG	Clone HA-tagged GnCTX

410

411 *Antibodies*

412 For immunoblot analyses the following primary antibodies (identifier, dilution) were used: anti-GFP
413 (Sigma G2544, 1:5000), anti-OROV (Gc detection; ATCC VR-1228AF, 1:1000), anti-HA (Cell Signaling
414 Technology C29F4, 1:2000), anti-GAPDH (GeneTex GTX28245, 1:10000) and anti-EEA1 (AbCam
415 Ab2900, 1:1000). The secondary antibodies were LI-COR IRDye 680T conjugated donkey anti-rabbit
416 (926-68023) or goat anti-mouse (926- 68020), or LI-COR IRDye 800CW conjugated donkey anti-rabbit
417 (926-32213) or goat anti-mouse (926-32210). For immunocytochemistry the following primary
418 antibodies (identifier, dilution) were used: anti-HA (Cell Signaling Technology, 1:1000), anti-GM130 (BD
419 Biosciences 610822, 1:1000) and anti-Calnexin2 (BD Biosciences 610523, 1:100). Secondary
420 antibodies were Alexa Fluor conjugated goat anti-mouse (A-21236, A-11001 and A-11031,
421 ThermoFisher), donkey anti-rabbit (A-10042, ThermoFisher) and goat anti-rabbit (A-11008,
422 ThermoFisher).

423 *OROV VLP assay and immunoblotting*

424 HEK293T cells were seeded at 2.5×10^5 cells per well in six well dishes. Cells were transfected by mixing
425 2 µg of DNA (split evenly by mass between the plasmids indicated) and 1.5 µg of branched
426 polyethylenimine (PEI; average MW ~25,000, Merck) in Opti-MEM (ThermoFisher), incubating at room
427 temperature for 20 min and then applying to cells. Cell culture medium was harvested after 48 h and
428 cleared of cellular debris by centrifugation at 800×g for 10 min at 4°C. Virus-like particles (VLPs) in the
429 supernatants were pelleted by centrifugation at 100,000×g at 4°C for 90 min using a TLA-55 rotor
430 (Beckman). The resultant pellets, containing VLPs, were resuspended and boiled in sodium dodecyl
431 sulfate-polyacrylamide gel electrophoresis (SDS-PAGE) sample buffer. Cell samples were harvested
432 by centrifugation and resuspended in lysis buffer (50 mM Tris pH 7.9, 150 mM NaCl, 1% (v/v) IGEPAL
433 CA-630 (a.k.a. NP-40), 1% (w/v) sodium deoxycholate) supplemented with protease inhibitor cocktail
434 (Roche) and incubated on ice for 30 min. Lysates were clarified by centrifugation at 20,000×g for 10
435 min at 4°C. The protein concentration in each lysate sample was normalized following quantification
436 using the BCA assay (ThermoFisher) and samples were boiled in SDS-PAGE sample buffer. Samples
437 were separated by SDS-PAGE using 10% or 15% (w/v) polyacrylamide gels and transferred to Protran
438 nitrocellulose membranes (Perkin Elmer) using the Mini-Trans blot system (BioRad) following the
439 manufacturer's protocol. After blocking in PBS with 5% (w/v) non-fat milk powder, membranes were
440 incubated with primary antibody at room temperature for 1 h or overnight at 4°C, washed, and then
441 incubated with the secondary antibody for 1 h at room temperature. Dried blots were visualized on an
442 Odyssey CLx infrared scanner (LI-COR).

443 For VLP isolation following drug treatment, HEK293T cells were transfected with a plasmid expressing
444 HA-tagged M polyprotein as described above. After 18 h, the culture medium was collected and VLPs
445 were isolated by ultracentrifugation as described above ("Before drugs"). The medium was replaced
446 with FreeStyle 293 medium (ThermoFisher) supplemented with brefeldin A (5 µg/mL), monensin (1 µM),
447 or MG132 (10 µM), and cells were incubated for a further 6 h before the supernatant and cell lysates
448 were harvested and processed as described above ("After drugs").

449 For VLP isolation from ecdysone-responsive stable cell lines, cells were seeded differently. Parental
450 and GFP-VPS4wt EcR293 cells were seeded at 5×10^6 cells per 9 cm dish, whereas GFP-VPS4E/Q
451 EcR293 cells (which grow more slowly) were seeded at 8×10^6 cells per 9 cm dish. Cells were
452 transfected with 7.7 µg of a plasmid expressing HA-tagged M polyprotein using TransIT-LT1 (Mirus)
453 and after 6 h the cells were treated with either DMSO or ponasterone A (1 µM). After 18 h of drug
454 treatment, the medium was refreshed using FreeStyle 293 medium (ThermoFisher). Cell lysates and
455 supernatants were harvested at 48 h post-transfection and processed as described above.

456 *Immunocytochemistry*

457 HeLa cells were seeded on glass coverslips at a density of 5×10^4 cells per well in 24 well dishes. Cells
458 were transfected with 250 ng of DNA (split evenly by mass between the plasmids indicated) using

459 TransIT-LT1 (Mirus) and incubated for 24 h before being transferred onto ice. Cells were washed with
460 ice-cold PBS and fixed with cold 250 mM HEPES pH 7.5, 4% (v/v) electron microscopy-grade
461 formaldehyde (PFA, Polysciences) for 10 min on ice before and then incubated with 20 mM HEPES pH
462 7.5, 8% (v/v) PFA at room temperature for a further 20 min. After washing with PBS, cells were
463 permeabilized by incubation with 0.1% saponin in PBS for 30 min before being incubated with blocking
464 buffer (5% [v/v] FBS, 0.1% saponin in PBS) for 30 min. Primary antibodies were diluted in blocking
465 buffer and incubated with coverslips for 2 h. Coverslips were washed five times with blocking buffer
466 before incubation for 1 h with the relevant secondary antibodies diluted in blocking buffer. Coverslips
467 were washed five times with blocking buffer, three times with 0.1% saponin in PBS, three times with
468 PBS, and finally with ultrapure water. Coverslips were mounted using Mowiol 4-88 (Merck) containing
469 200 nM 4′,6-diamidino-2-phenylindole (DAPI) and allowed to set overnight. Cells were analyzed with
470 an Olympus IX81 fluorescence microscope. Images were captured using a Reitga 2000R charge-
471 coupled device camera and processed using Fiji ImageJ software (23).

472 For the drug treatment assay, HeLa cells were seeded on glass coverslips at a density of 5×10^4 cells
473 per well in 24 well dishes and transfected with a plasmid expressing HA-tagged M polyprotein. After
474 18 h the culture medium was replaced and supplemented with brefeldin A (5 µg/mL), monensin (1 µM),
475 or MG132 (10 µM). After 6 h of drug treatment, cells were fixed and processed as described above.

476 Ecdysone-responsive stable cell lines were seeded on poly-D-lysine treated glass coverslips at a
477 density of 2×10^4 cells per well in 24 well dishes. Cells were transfected with 250 ng of a plasmid
478 expressing HA-tagged M polyprotein using TransIT-LT1 (Mirus) and after 6 h cells were treated with
479 ponasterone A (1 µM) or DMSO. After 18 h of drug treatment, cells were fixed and processed as
480 described above.

481 **Acknowledgements**

482 The authors thank Susanna Colaco for superb technical assistance. This work was supported by
483 doctoral studentship and travelling fellowship from the Fundação de Amparo à Pesquisa do Estado de
484 São Paulo (FAPESP; 2016/18356-4 and 2019/02945-9) to NSB, by a FAPESP Pump Priming award
485 (2019/02418-9) to LLPdS, by a Biotechnology and Biological Sciences Research Council
486 (BBSRC)/FAPESP pump priming award (BB/S018670/1) to CMC, LLPdS and SCG, and by a Sir Henry
487 Dale Fellowship co-funded by the Royal Society and the Wellcome Trust (098406/Z/12/B) to SCG.

488 **References**

489 1. Sakkas H, Bozidis P, Franks A, Papadopoulou C. 2018. Oropouche Fever: A Review. Viruses
490 10:175.

491 2. Romero-Alvarez D, Escobar LE. 2018. Oropouche fever, an emergent disease from the
492 Americas. Microbes Infect 20:135-146.

493 3. Gutierrez B, Wise EL, Pullan ST, Logue CH, Bowden TA, Escalera-Zamudio M, Trueba G,
494 Nunes MRT, Faria NR, Pybus OG. 2020. Evolutionary Dynamics of Oropouche Virus in South
495 America. J Virol 94:e01127-19.

496 4. Elliott RM. 2014. Orthobunyaviruses: recent genetic and structural insights. Nat Rev Microbiol
497 12:673-85.

498 5. Barbosa NS, Mendonça LR, Dias MVS, Pontelli MC, da Silva EZM, Criado MF, da Silva-
499 Januário ME, Schindler M, Jamur MC, Oliver C, Arruda E, daSilva LLP. 2018. ESCRT
500 machinery components are required for Orthobunyavirus particle production in Golgi
501 compartments. PLoS Pathog 14:e1007047.

502 6. Salanueva IJ, Novoa RR, Cabezas P, López-Iglesias C, Carrascosa JL, Elliott RM, Risco C.
503 2003. Polymorphism and structural maturation of bunyamwera virus in Golgi and post-Golgi
504 compartments. J Virol 77:1368-81.

505 7. Lappin DF, Nakitare GW, Palfreyman JW, Elliott RM. 1994. Localization of Bunyamwera
506 bunyavirus G1 glycoprotein to the Golgi requires association with G2 but not with NSm. J Gen
507 Virol 75:3441-51.

508 8. Christ L, Raiborg C, Wenzel EM, Campsteijn C, Stenmark H. 2017. Cellular Functions and
509 Molecular Mechanisms of the ESCRT Membrane-Scission Machinery. Trends Biochem Sci
510 42:42-56.

511 9. Maity S, Caillat C, Miguet N, Sulbaran G, Effantin G, Schoehn G, Roos WH, Weissenhorn W.
512 2019. VPS4 triggers constriction and cleavage of ESCRT-III helical filaments. Sci Adv
513 5:eaau7198.

514 10. Schöneberg J, Pavlin MR, Yan S, Righini M, Lee IH, Carlson LA, Bahrami AH, Goldman DH,
515 Ren X, Hummer G, Bustamante C, Hurley JH. 2018. ATP-dependent force generation and
516 membrane scission by ESCRT-III and Vps4. Science 362:1423-1428.

517 11. Effantin G, Dordor A, Sandrin V, Martinelli N, Sundquist WI, Schoehn G, Weissenhorn W. 2013.
518 ESCRT-III CHMP2A and CHMP3 form variable helical polymers in vitro and act synergistically
519 during HIV-1 budding. Cell Microbiol 15:213-26.

520 12. Freed EO. 2002. Viral late domains. J Virol 76:4679-87.

521 13. Votteler J, Sundquist WI. 2013. Virus budding and the ESCRT pathway. Cell Host Microbe
522 14:232-41.

523 14. Tabata K, Arimoto M, Arakawa M, Nara A, Saito K, Omori H, Arai A, Ishikawa T, Konishi E,
524 Suzuki R, Matsuura Y, Morita E. 2016. Unique Requirement for ESCRT Factors in Flavivirus
525 Particle Formation on the Endoplasmic Reticulum. Cell Rep 16:2339-47.

526 15. Vietri M, Radulovic M, Stenmark H. 2020. The many functions of ESCRTs. Nat Rev Mol Cell
527 Biol 21:25-42.

528 16. Watanabe S, Watanabe T, Noda T, Takada A, Feldmann H, Jasenosky LD, Kawaoka Y. 2004.
529 Production of novel Ebola virus-like particles from cDNAs: an alternative to Ebola virus
530 generation by reverse genetics. J Virol 78:999-1005.

531 17. Strecker T, Eichler R, Meulen J, Weissenhorn W, Dieter Klenk H, Garten W, Lenz O. 2003.
532 Lassa virus Z protein is a matrix protein and sufficient for the release of virus-like particles. J
533 Virol 77:10700-5.

534 18. Roldão A, Mellado MC, Castilho LR, Carrondo MJ, Alves PM. 2010. Virus-like particles in
535 vaccine development. Expert Rev Vaccines 9:1149-76.

536 19. Acuña R, Cifuentes-Muñoz N, Márquez CL, Bulling M, Klingström J, Mancini R, Lozach PY,
537 Tischler ND. 2014. Hantavirus Gn and Gc glycoproteins self-assemble into virus-like particles.
538 J Virol 88:2344-8.

539 20. Overby AK, Popov V, Neve EP, Pettersson RF. 2006. Generation and analysis of infectious
540 virus-like particles of uukuniemi virus (bunyaviridae): a useful system for studying bunyaviral
541 packaging and budding. J Virol 80:10428-35.

542 21. Acrani GO, Tilston-Lunel NL, Spiegel M, Weidmann M, Dilcher M, Andrade da Silva DE, Nunes
543 MR, Elliott RM. 2015. Establishment of a minigenome system for Oropouche virus reveals the
544 S genome segment to be significantly longer than reported previously. J Gen Virol 96:513-23.
545 22. Kohl A, Hart TJ, Noonan C, Royall E, Roberts LO, Elliott RM. 2004. A bunyamwera virus
546 minireplicon system in mosquito cells. J Virol 78:5679-85.
547 23. Shi X, Botting CH, Li P, Niglas M, Brennan B, Shirran SL, Szemiel AM, Elliott RM. 2016.
548 Bunyamwera orthobunyavirus glycoprotein precursor is processed by cellular signal peptidase
549 and signal peptide peptidase. Proc Natl Acad Sci U S A 113:8825-30.
550 24. Tilston-Lunel NL, Acrani GO, Randall RE, Elliott RM. 2015. Generation of Recombinant
551 Oropouche Viruses Lacking the Nonstructural Protein NSm or NSs. J Virol 90:2616-27.
552 25. Nielsen H. 2017. Predicting Secretory Proteins with SignalP. Methods Mol Biol 1611:59-73.
553 26. Fujiwara T, Oda K, Yokota S, Takatsuki A, Ikehara Y. 1988. Brefeldin A causes disassembly of
554 the Golgi complex and accumulation of secretory proteins in the endoplasmic reticulum. J Biol
555 Chem 263:18545-52.
556 27. Mollenhauer HH, Morré DJ, Rowe LD. 1990. Alteration of intracellular traffic by monensin;
557 mechanism, specificity and relationship to toxicity. Biochim Biophys Acta 1031:225-46.
558 28. Mimnaugh EG, Chen HY, Davie JR, Celis JE, Neckers L. 1997. Rapid deubiquitination of
559 nucleosomal histones in human tumor cells caused by proteasome inhibitors and stress
560 response inducers: effects on replication, transcription, translation, and the cellular stress
561 response. Biochemistry 36:14418-29.
562 29. Crump CM, Yates C, Minson T. 2007. Herpes simplex virus type 1 cytoplasmic envelopment
563 requires functional Vps4. J Virol 81:7380-7.
564 30. Pawliczek T, Crump CM. 2009. Herpes simplex virus type 1 production requires a functional
565 ESCRT-III complex but is independent of TSG101 and ALIX expression. J Virol 83:11254-64.
566 31. Shi X, Lappin DF, Elliott RM. 2004. Mapping the Golgi targeting and retention signal of
567 Bunyamwera virus glycoproteins. J Virol 78:10793-802.
568 32. Overby AK, Pettersson RF, Neve EP. 2007. The glycoprotein cytoplasmic tail of Uukuniemi
569 virus (Bunyaviridae) interacts with ribonucleoproteins and is critical for genome packaging. J
570 Virol 81:3198-205.
571 33. Shi X, Kohl A, Li P, Elliott RM. 2007. Role of the cytoplasmic tail domains of Bunyamwera
572 orthobunyavirus glycoproteins Gn and Gc in virus assembly and morphogenesis. J Virol
573 81:10151-60.
574 34. Shi X, Brauburger K, Elliott RM. 2005. Role of N-linked glycans on bunyamwera virus
575 glycoproteins in intracellular trafficking, protein folding, and virus infectivity. J Virol 79:13725-
576 34.
577 35. Sciaky N, Presley J, Smith C, Zaal KJ, Cole N, Moreira JE, Terasaki M, Siggia E, Lippincott-
578 Schwartz J. 1997. Golgi tubule traffic and the effects of brefeldin A visualized in living cells. J
579 Cell Biol 139:1137-55.
580 36. Kaufman RJ. 1999. Stress signaling from the lumen of the endoplasmic reticulum: coordination
581 of gene transcriptional and translational controls. Genes Dev 13:1211-33.
582 37. Novoa RR, Calderita G, Cabezas P, Elliott RM, Risco C. 2005. Key Golgi factors for structural
583 and functional maturation of bunyamwera virus. J Virol 79:10852-63.
584 38. Patnaik A, Chau V, Wills JW. 2000. Ubiquitin is part of the retrovirus budding machinery. Proc
585 Natl Acad Sci U S A 97:13069-74.
586 39. De Franceschi N, Alqabandi M, Miguet N, Caillat C, Mangenot S, Weissenhorn W, Bassereau
587 P. 2018. The ESCRT protein CHMP2B acts as a diffusion barrier on reconstituted membrane
588 necks. J Cell Sci 132.
589 40. Morita E, Sandrin V, McCullough J, Katsuyama A, Baci Hamilton I, Sundquist WI. 2011.
590 ESCRT-III protein requirements for HIV-1 budding. Cell Host Microbe 9:235-242.
591